XI International Conference on Computational Plasticity. Fundamentals and Applications
COMPLAS XI
E. Oñate, D.R.J. Owen, D. Peric and B. Suárez (Eds)

CYCLIC VISCOELASTOPLASTICITY AND FATIGUE FRACTURE OF POLYMER COMPOSITES

ALEKSEY D. DROZDOV*

*Department of Plastics Technology
Danish Technological Institute
Gregersensvej 1, 2630 Taastrup, Denmark
e-mail: Aleksey.Drozdov@teknologisk.dk

Key words: Viscoelastoplasticity, Polymer/clay hybrids, Ratcheting, Fatigue

Abstract. Observations are reported on isotactic polypropylene/nanoclay hybrids with various concentrations of filler ranging from 0 to 5 wt.% in cyclic tensile tests with a stress–controlled program (ratcheting between minimum stresses $\sigma^{\min}$ and maximum stresses $\sigma^{\max}$). A pronounced effect of filler is demonstrated: reinforcement of polypropylene with 1 wt.% of nanoclay results in reduction of maximum and minimum strains per cycle by several times and growth of number of cycles to failure by an order of magnitude. To rationalize these findings, a constitutive model is developed in cyclic viscoelastoplasticity of polymer nanocomposites. Adjustable parameters in the stress–strain relations are found by fitting experimental data in relaxation tests and cyclic tests. It is demonstrated that the model correctly predicts growth of maximum and minimum strains per cycle with number of cycles and can be applied for evaluation of fatigue failure of nanocomposites.

1 INTRODUCTION

This paper is concerned with experimental investigation and constitutive modeling of the viscoelastic and viscoplastic responses of polymer/clay nanocomposites in tensile cyclic tests with stress-controlled programs.

A number of studies on the mechanical behavior of polymer/clay hybrids reveal noticeable improvement of their properties due to the presence of nanoparticles [1, 2, 3]. This enhancement remains, however, rather modest compared with what has been expected from the effect of reinforcement a decade ago [3]. Keeping in mind these discrepancies between expected and real mechanical properties of nanohybrids in conventional tensile tests, it seems natural to focus on more sophisticated deformation programs, where the effect of nanofiller becomes significant for applications. This approach was initiated in [4, 5, 6] by demonstrating that reinforcement of polymers with nanoparticles dramatically enhanced creep resistance and in [7, 8] by revealing a similar effect for ratcheting strain in cyclic tests.

The objective of this study is threefold: (i) to demonstrate that reinforcement of polypropylene with nanoclay results in a strong decrease in maximum and minimum strains per cycle observed in uniaxial tensile cyclic tests with a stress-controlled program, (ii) to develop a constitutive model in cyclic viscoelastoplasticity of polymer nanocomposites that describes this phenomenon, and (iii) to rationalize physical mechanisms responsible for the improvement of fatigue resistance by comparison of material parameters in the stress–strain relations.

2 EXPERIMENTAL RESULTS

Nanocomposites with isotactic polypropylene as a matrix [Moplen HP 400R (Albis Plastic Scandinavia AB, Sweden)], maleic anhydride grafted polypropylene as a compatibilizer [Eastman G 3015 (Eastman Chemical Company, USA)], and organically modified montmorillonite nanoclay as a filler [Delitte 67G (Laviosa Chimica Mineraria S.p.A., Italy)] were manufactured in a two-step process described in [6]. Nanohybrids with clay/compabilizer proportion 1:2 and clay contents $\chi = 0$, 1, 3, and 5 wt.% were prepared by means of twin-screw extruder Brabender PL2000. Dumbbell specimens for tensile tests (ASTM standard D638) were molded by using injection-molding machine Arburg 320C.

Uniaxial tensile tests were performed at room temperature by means of universal testing machine Instron–5569 equipped with an electro-mechanical sensor for control of longitudinal strains. The engineering stress σ was determined as the ratio of axial force to cross-sectional area of undeformed specimens.

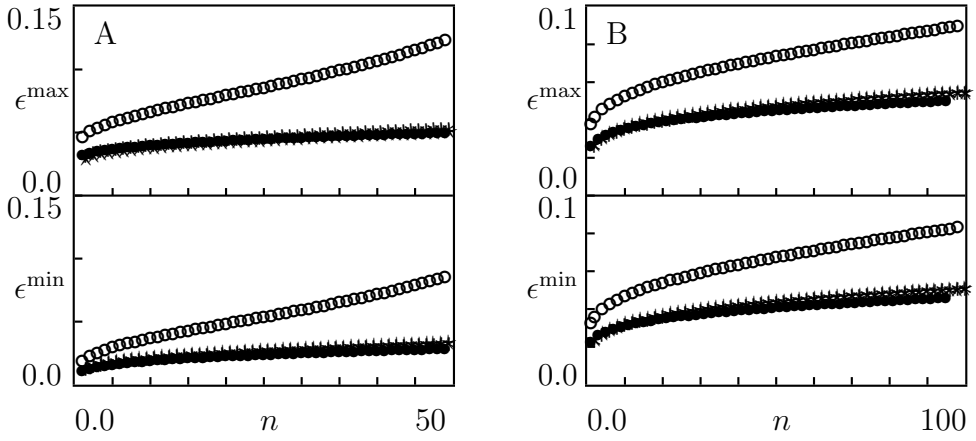

Figure 1: Maximum $\epsilon^{\max}$ and minimum $\epsilon^{\min}$ strains per cycle versus number of cycles n. Symbols: experimental data in cyclic tests with $\dot{d} = 10$ mm/min, $\sigma^{\max} = 25$ MPa, $\sigma^{\min} = 20$ MPa (A) and $\dot{d} = 100$ mm/min, $\sigma^{\max} = 30$ MPa, $\sigma^{\min} = 10$ MPa (B) on nanocomposites with clay content χ wt.% ($\circ$ $\chi = 0$, $\bullet$ $\chi = 1$, $*$ $\chi = 3$, $\star$ $\chi = 5$).

Two series of experiments were conducted at room temperature. The first was aimed to choose deformation programs that ensure the most pronounced effect of reinforcement. It involved five ratcheting tests with various maximum stresses $\sigma^{\max}$, minimum stresses

$\sigma^{\min}$ and strain rates $\dot{\epsilon}$. In each test, a specimen was stretched with a fixed cross-head speed $\dot{d}$ up to a maximum stress $\sigma^{\max}$, retracted down to a minimum stress $\sigma^{\min}$ with the same cross-head speed, reloaded up to the maximum stress $\sigma^{\max}$ with the cross-head speed $\dot{d}$, unloaded down to the minimum stress $\sigma^{\min}$ with the same cross-head speed, etc. Some experimental data in cyclic tests are reported in Figure 1, where maximum strain per cycle $\epsilon^{\max}$ and minimum strain per cycle $\epsilon^{\min}$ are plotted versus number of cycles n. Observations show that for all experimental conditions, reinforcement of polypropylene with nanoclay results in noticeable reduction in $\epsilon^{\max}$ and $\epsilon^{\min}$. The strongest improvement of fatigue resistance is reached when concentration of filler equals 1 wt.%.

The other series of tests was carried out for identification of parameters in constitutive equations. It involved cyclic tests with a stress-controlled program and relaxation tests. Each test was carried out on a new sample and repeated by twice to confirm reproducibility of measurements. Based on observations in the first series of tests, we confine ourselves to the analysis of nanocomposites with $\chi = 0$ and 1 wt.%.

Ratcheting tests were performed with $\dot{d} = 100$ mm/min, $\sigma^{\max} = 30$ MPa, and $\sigma^{\min} = 20$ MPa. Experimental stress–strain curves (16 cycles of loading–retraction) and diagrams $\epsilon^{\max}(n)$, $\epsilon^{\min}(n)$ are depicted in Figure 2.

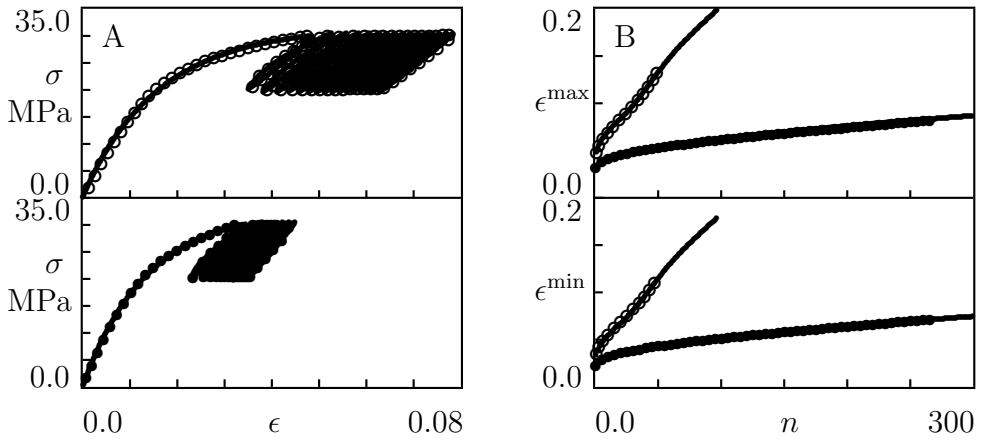

Figure 2: A—Stress σ versus strain ϵ. B—Maximum $\epsilon^{\max}$ and minimum $\epsilon^{\min}$ strains versus number of cycles n. Circles: experimental data in cyclic tests on nanocomposites with $\chi = 0$ ($\circ$) and $\chi = 1$ ($\bullet$) wt.%. Solid lines: results of numerical simulation.

Relaxation tests were conducted with a fixed strain $\epsilon = 0.1$. In each test, a specimen was stretched with $\dot{d} = 100$ mm/min up to the required strain. Afterwards, ϵ was preserved constant, and a decrease in stress σ was monitored as a function of time t. Following the ASTM protocol E–328 for short-term relaxation tests, duration of relaxation tests $t_{\rm rel} = 20$ min was chosen.

Observations in relaxation tests are reported in Figure 3, where engineering stress σ is depicted versus relaxation time $t' = t - t_0$ (t_0 stands for the instant when relaxation starts). Following common practice, the semi-logarithmic plot is chosen with $\log = \log_{10}$.

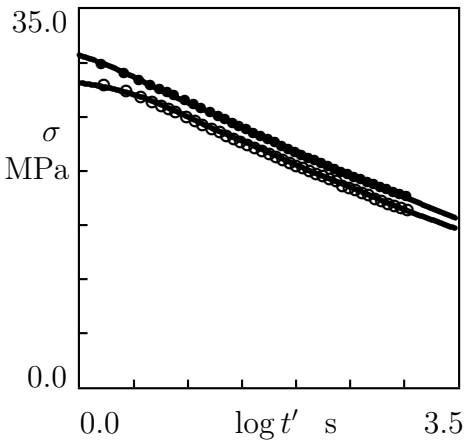

Figure 3: Stress σ versus relaxation time t'. Symbols: experimental data in relaxation tests on nanocomposites with $\chi = 0$ ($\circ$) and $\chi = 1$ ($\bullet$) wt.%. Solid lines: results of numerical simulation.

Figure 3 shows that the viscoelastic response of nanocomposites is weakly affected by clay content.

3 CONSTITUTIVE MODEL

With reference to the homogenization concept [9], a nanocomposite with a complicated microstructure (a semicrystalline matrix reinforced with randomly distributed clay platelets and their stacks) is replaced with an equivalent isotropic medium, whose mechanical response resembles that of the composite. An incompressible, inhomogeneous, transient, non-affine network of polymer chains bridged by junctions is chosen as the equivalent continuum. The incompressibility hypothesis is confirmed by observations in uniaxial tensile tests with cross-head speed 200 mm/min, where longitudinal and transverse strains were measured simultaneously. Poisson's ratios of nanocomposites with $\chi = 0$ and 1 wt.% read 0.498 and 0.476, respectively.

3.1 Kinematics of plastic deformations

To describe plastic flow in the equivalent medium at small strains, the strain tensor for macro-deformation $\hat{\epsilon}$ is presented as the sum of elastic strain tensor $\hat{\epsilon}_{\rm e}$ and plastic strain tensor $\hat{\epsilon}_{\rm p}$

$$\hat{\epsilon} = \hat{\epsilon}_{\rm e} + \hat{\epsilon}_{\rm p}. \tag{1}$$

With reference to conventional phenomenological models with two plastic elements connected in series, the plastic strain tensor $\hat{\epsilon}_{\rm p}$ is split into the sum of two components

$$\hat{\epsilon}_{\rm p} = \hat{\epsilon}_{\rm p}^{(1)} + \hat{\epsilon}_{\rm p}^{(2)}. \tag{2}$$

The tensors $\hat{\epsilon}_{\rm p}^{(1)}$ and $\hat{\epsilon}_{\rm p}^{(2)}$ are presumed to describe inelastic deformations in the matrix and inclusions, respectively.

The strain rate for plastic deformation in the matrix is proportional to strain rate for macro-deformation

$$\frac{\mathrm{d}\hat{\epsilon}_{\mathrm{p}}^{(1)}}{\mathrm{d}t} = \phi \frac{\mathrm{d}\hat{\epsilon}}{\mathrm{d}t}, \tag{3}$$

where the non-negative function ϕ (i) vanishes in the undeformed state (which means that no plastic deformation occurs at very small strains), (ii) monotonically grows under active loading and decreases under retraction (which reflects stress-induced acceleration of plastic flow), and (iii) reaches its ultimate value $\phi_\infty = 1$ at large strains (when the rates of plastic deformation and macro-deformation coincide). Changes in ϕ with time are governed by the differential equation

$$\frac{\mathrm{d}\phi}{\mathrm{d}t} = \pm a(1-\phi)^2 \dot{\epsilon}, \qquad \phi(0) = 0, \tag{4}$$

where the signs "+" and "−" correspond to loading and retraction, respectively, $\dot{\epsilon} = \left(\frac{2}{3}\frac{\mathrm{d}\hat{\epsilon}}{\mathrm{d}t} : \frac{\mathrm{d}\hat{\epsilon}}{\mathrm{d}t}\right)^{\frac{1}{2}}$ stands for the equivalent strain rate for macro-deformation, and the coefficient a adopts different values a_1 and a_2 under active deformation and unloading. For uniaxial tension, loading and unloading are determined unambiguously. For an arbitrary three-dimensional deformation, these processes are defined following [10, 11].

3.2 Heterogeneity of the network

An inhomogeneous transient polymer network is composed of meso-domains with various activation energies for rearrangement of chains. The rate of separation of active chains from their junctions in a meso-domain with activation energy u is governed by the Eyring equation $\Gamma = \gamma \exp[-u/(k_B T)]$, where γ is an attempt rate, k_B denotes Boltzmann's constant, and T stands for absolute temperature. Introducing dimensionless activation energy $v = u/(k_B T)$, we obtain

$$\Gamma(v) = \gamma \exp(-v). \tag{5}$$

Denote by N concentration of active chains in the equivalent network [12]. The number of active chains $n_0(v)$ in meso-domains with activation energy v (per unit volume) reads

$$n_0(v) = N f(v), \tag{6}$$

where $f(v)$ stands for a distribution function of meso-domains. With reference to the random energy model [13], the quasi-Gaussian expression is accepted for this function

$$f(v) = f_0 \exp\Big[-\frac{1}{2}\Big(\frac{v}{\Sigma}\Big)^2\Big] \qquad (v \geq 0), \qquad f(v) = 0 \qquad (v < 0). \tag{7}$$

Parameters N, γ, and Σ are assumed to be independent of mechanical factors. The pre-factor f_0 is determined from the normalization condition $\int_0^\infty f(v)\mathrm{d}v = 1$.

3.3 Rearrangement of chains

Rearrangement of a temporary network is described by a function $n(t,\tau,v)$ which equals the number (per unit volume) of temporary chains at time $t \geq 0$ that have returned into the active state before instant $\tau \leq t$ and belong to a meso-domain with energy v. The number of active chains in meso-domains with energy v at time t reads

$$n(t,t,v) = n_0(v). \tag{8}$$

The number of chains that were active at the initial instant $t = 0$ and have not separated from their junctions until time t is $n(t,0,v)$. The number of chains that were active at the initial instant and detach from their junctions within the interval $[t, t+\mathrm{d}t]$ equals $-\partial n/\partial t(t,0,v)\,\mathrm{d}t$, the number of dangling chains that return into the active state within the interval $[\tau, \tau+\mathrm{d}\tau]$ is given by $P(\tau,v)\mathrm{d}\tau$ with

$$P(\tau,v) = \frac{\partial n}{\partial \tau}(t,\tau,v)\Big|_{t=\tau}, \tag{9}$$

and the number of chains that merged (for the last time) with the network within the interval $[\tau, \tau+\mathrm{d}\tau]$ and detach from their junctions within the interval $[t, t+\mathrm{d}t]$ reads $-\partial^2 n/\partial t\partial\tau(t,\tau,v)\,\mathrm{d}t\mathrm{d}\tau$. Detachment of chains from their junctions is described by the kinetic equations

$$\frac{\partial n}{\partial t}(t,0,v) = -\Gamma(v)n(t,0,v), \qquad \frac{\partial^2 n}{\partial t\partial\tau}(t,\tau,v) = -\Gamma(v)\frac{\partial n}{\partial\tau}(t,\tau,v), \tag{10}$$

which mean that the number of active chains separating from their junctions per unit time is proportional to the total number of active chains in an appropriate meso-domain. Integration of Eq. (10) with initial conditions (6), (8), and (9) implies that

$$n(t,0,v) = Nf(v)\exp[-\Gamma(v)t], \qquad \frac{\partial n}{\partial\tau}(t,\tau,v) = Nf(v)\Gamma(v)\exp[-\Gamma(v)(t-\tau)]. \tag{11}$$

3.4 Stress–strain relations

The strain energy of an active chain reads

$$w = \frac{1}{2}\bar{\mu}\hat{\epsilon}_{\mathrm{e}} : \hat{\epsilon}_{\mathrm{e}}, \tag{12}$$

where $\bar{\mu}$ stands for rigidity of a chain, and the colon denotes convolution of tensors. The strain energy of a chain that has last returned into the active state at instant $\tau < t$ is determined by Eq. (12), where $\hat{\epsilon}_{\mathrm{e}}(t)$ is replaced with $\hat{\epsilon}_{\mathrm{e}}(t) - \hat{\epsilon}_{\mathrm{e}}(\tau)$. The strain energy density (per unit volume) of individual chains in a transient polymer network is given by

$$\begin{aligned} W_1(t) \;=\; & \frac{1}{2}\bar{\mu}\Big[\int_0^\infty n(t,0,v)\,\mathrm{d}v\;\hat{\epsilon}_{\mathrm{e}}(t) : \hat{\epsilon}_{\mathrm{e}}(t) \\ & + \int_0^\infty \mathrm{d}v \int_0^t \frac{\partial n}{\partial\tau}(t,\tau,v)\Big(\hat{\epsilon}_{\mathrm{e}}(t) - \hat{\epsilon}_{\mathrm{e}}(\tau)\Big) : \Big(\hat{\epsilon}_{\mathrm{e}}(t) - \hat{\epsilon}_{\mathrm{e}}(\tau)\Big)\,\mathrm{d}\tau\Big]. \end{aligned} \tag{13}$$

The first term in Eq. (13) equals the energy of active chains that have not been rearranged within the interval $[0,t]$. The other term expresses the energy of chains that have last merged with the network at various instants $\tau \in [0,t]$ and remained active until instant t.

At the nth cycle of cyclic deformation, the energy of interaction between chains and nanofiller is described by the analog of Eq. (12)

$$W_2 = \frac{1}{2}\tilde{\mu}\Bigl(\hat{\epsilon}_{\rm p}^{(2)} : \hat{\epsilon}_{\rm p}^{(2)} - \hat{\epsilon}_{\rm p}^{(2)0} : \hat{\epsilon}_{\rm p}^{(2)0}\Bigr), \tag{14}$$

where the tensor $\hat{\epsilon}_{\rm p}^{(2)}$ describes irreversible deformation in stacks of clay platelets, $\hat{\epsilon}_{\rm p}^{(2)0}$ coincides with $\hat{\epsilon}_{\rm p}^{(2)}$ at the instant when the strain rate for macro-deformation changes its sign, and $\tilde{\mu} > 0$ accepts different values $\tilde{\mu}_1$ and $\tilde{\mu}_2$ under loading and unloading, respectively. It is worth noting that the last term in Eq. (14) does not affect constitutive equations as the strain energy is determined up to an arbitrary additive constant.

The strain energy density of the equivalent network equals the sum of strain energies of individual chains and the energy of their interaction

$$W = W_1 + W_2. \tag{15}$$

For isothermal volume-preserving deformation, the Clausius–Duhem inequality reads

$$\frac{{\rm d}Q}{{\rm d}t} = -\frac{{\rm d}W}{{\rm d}t} + \hat{\sigma}' : \frac{{\rm d}\hat{\epsilon}}{{\rm d}t} \geq 0, \tag{16}$$

where Q stands for internal dissipation per unit volume, and $\hat{\sigma}'$ denotes deviatoric part of the stress tensor $\hat{\sigma}$. Combining Eqs. (12)–(16) and using Eq. (11), we arrive at the stress–strain relation

$$\hat{\sigma}(t) = -p(t)\hat{I} + \mu\Bigl(1-\phi(t)\Bigr)\Bigl[\hat{\epsilon}_{\rm e}(t) - \int_0^\infty f(v){\rm d}v \int_0^t \Gamma(v)\exp\Bigl(-\Gamma(v)(t-\tau)\Bigr)\hat{\epsilon}_{\rm e}(\tau){\rm d}\tau\Bigr], \tag{17}$$

where $\mu = \bar{\mu}N$, p is an unknown pressure, and $\hat{I}$ stands for the unit tensor. Inequality (16) is satisfied provided that

$$\frac{{\rm d}\hat{\epsilon}_{\rm p}^{(2)}}{{\rm d}t}(t) = S\dot{\epsilon}\Bigl[\hat{\epsilon}_{\rm e}(t) - R\hat{\epsilon}_{\rm p}^{(2)}(t) - \int_0^\infty f(v)\hat{Z}(t,v){\rm d}v\Bigr], \tag{18}$$

where the coefficients $R = \tilde{\mu}/\mu$ and S adopts different (but constant) values R_1, S_1 and R_2, S_2 under loading and unloading, respectively. The function $\hat{Z}(t,v) = \int_0^t \Gamma(v)\exp[-\Gamma(v)(t-\tau)]\hat{\epsilon}_{\rm e}(\tau){\rm d}\tau$ is governed by the differential equation

$$\frac{\partial \hat{Z}}{\partial t}(t,v) = \Gamma(v)[\hat{\epsilon}_{\rm e}(t) - \hat{Z}(t,v)], \qquad \hat{Z}(0,v) = 0. \tag{19}$$

Stress–strain relation (17) together with kinematic equations (1), (2) and kinetic equations (3), (4), (18), and (19) provide constitutive equations for the viscoelastoplastic behavior of

polymer nanocomposites under cyclic deformation. These relations involve three material constants, μ, γ, Σ, and six adjustable functions, a_1, a_2, R_1, R_2, S_1, S_2, with the following meaning: (i) μ stands for an elastic modulus of a polymer nanocomposite, (ii) γ and Σ characterize its linear viscoelastic behavior, (iii) a_1 and a_2 describe irreversible deformation in the matrix under loading and unloading, (iv) R_1, S_1 and R_2, S_2 characterize plastic flow in stacks of clay platelets under active deformation and retraction.

3.5 Adjustable functions

Evolution of material functions under cyclic deformation is described by the following scenario.

The coefficients S_1 and S_2 reach their ultimate values within the first two cycles. For active loading of a virgin specimen, $S_1 = 0$, while for subsequent reloadings, $S_1 = S_{1\infty}$. Similarly, S_2 adopts some value S_{20} for the first retraction, whereas for subsequent unloadings, $S_2 = S_{2\infty}$. The entire set of these coefficients is determined by three constants: S_{20}, $S_{1\infty}$, and $S_{2\infty}$.

The coefficients a_1 and a_2 are equilibrated within first 5–6 cycles. In subsequent cycles of loading–retraction, they adopt their ultimate values $a_{1\infty} = a_{2\infty} = a_\infty$.

The coefficient R_2 is a decreasing function of intensity of plastic strain $\epsilon_{\rm p} = \left(\frac{2}{3}\hat{\epsilon}_{\rm p} : \hat{\epsilon}_{\rm p}\right)^{\frac{1}{2}}$ at instants when transition occurs from active loading to unloading ($\epsilon_{\rm p} = \epsilon_{\rm p}^{\max}$). This function obeys the differential equation

$$\frac{{\rm d}R_2}{{\rm d}\epsilon_{\rm p}^{\max}} = -A_2 R_2^2, \tag{20}$$

where A_2 is a positive coefficient.

The coefficient R_1 is split into the sum of two components

$$R_1 = r + R, \tag{21}$$

where evolution of r is induced by damage accumulation in stacks of clay platelets, and R characterizes changes in energy of inter-particle interaction driven by plastic flow.

For a stress-controlled deformation program with fixed maximum and minimum stresses, number of cycles n serves as a measure of damage accumulation. The effect of this measure on r is described by the phenomenological equation

$$r = r_0 \exp(-\alpha n), \tag{22}$$

where r_0 and α are positive constants. The decay in r with n occurs rather rapidly, which implies that r vanishes after a transition period (about 10 cycles).

A decrease in R with plastic strain is governed by the differential equation

$$\frac{{\rm d}R}{{\rm d}\epsilon_{\rm p}^{\min}} = A_1(R_\infty - R), \tag{23}$$

where A_1 and R_∞ are adjustable parameters, and $\epsilon_{\rm p}^{\rm min}$ stands for intensity of plastic strain $\epsilon_{\rm p}$ at instants when transition occurs from retraction to reloading.

After an initial transition period, the viscoelastoplastic response of a nanocomposite is determined by 10 material constants: μ, γ, Σ, A_1, A_2, a_∞, r_∞, R_∞, $S_{1\infty}$, and $S_{2\infty}$. Although this number is not small, it is substantially lower than the number of adjustable parameters in conventional constitutive models for multi-cycle loading [15, 16, 17]. An important advantage of the present approach is that the material constants are found by fitting loading and unloading paths of stress–strain diagrams step by step, which implies that not more than 3 parameters are determined by matching each set of observations.

4 FITTING OF OBSERVATIONS

Adjustable parameters in the constitutive equations are found by approximation of the experimental data in Figures 2 and 3 following the algorithm described in [14]. Each set of observations is matched separately. Material constants in the stress–strain relations are listed in Table 1.

Table 1: Adjustable parameters for polypropylene/nanoclay hybrids

Parameter	$\chi = 0$	$\chi = 1$	Parameter	$\chi = 0$	$\chi = 1$
E (GPa)	2.04	2.48	γ ($\rm s^{-1}$)	0.10	0.34
Σ	10.9	11.7	$S_{1\infty}$	4.70	14.4
S_{20}	12.9	12.7	$S_{2\infty}$	19.6	26.5
a_∞	9.13	9.56	A_1	51.5	73.0
R_∞	6.84	2.53	A_2	58.0	44.1

Figure 2 demonstrates good agreement between the observations in cyclic tests (cycles) and the results of numerical analysis (solid lines). To reveal the quality of fitting, the experimental stress–strain curves for the first two cycles and the 16th cycle are reported in Figure 4 together with results of simulation. This figure confirms that accuracy of approximation is not reduced with number of cycles.

5 DISCUSSION

To understand physical mechanisms responsible for substantial reduction in ratcheting strain due to reinforcement of polypropylene, we compare adjustable parameters listed in Table 1.

Reinforcement of polypropylene with 1 wt.% of nanoclay results in an increase in Young's modulus E by 22%, which reflects improvement of its elastic properties.

The effect of filler on viscoelastic properties appears to be of secondary importance. It is observed as a weak broadening of the relaxation spectrum (Σ grows by 7%) and an increase in the rate of rearrangement γ (by 3 times). The growth of relaxation rate

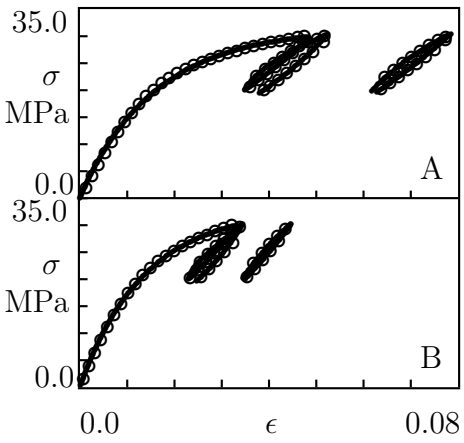

Figure 4: Stress σ versus strain ϵ. Circles: experimental data in cyclic tests (the first two cycles and the 16th cycle) with $\sigma^{\max} = 30$ MPa and $\sigma^{\min} = 20$ MPa on nanocomposites with $\chi = 0$ (A) and $\chi = 1$ (B) wt.%. Solid lines: results of numerical simulation.

does not seem dramatic, as $\log \gamma$ is conventionally employed in the Eyring or Arrhenius relations.

The equilibrium rate of viscoplastic flow in the polymer matrix a_∞ remains practically unaffected by clay content (it increases by less than 5% due to the presence of nanoclay).

Rather substantial changes are observed in coefficients $S_{1\infty}$ and $S_{2\infty}$ that reflect evolution of plastic strain tensor $\hat{\epsilon}_{\rm p}^{(2)}$ (which serves as a measure of irreversible deformations in stacks of clay platelets). Reinforcement of polypropylene with 1 wt.% of nanoclay results in an increase in $S_{1\infty}$ by 3 times and in $S_{2\infty}$ by 35%. Keeping in mind that S_1 and S_2 are proportional to rates of plastic flow under loading and unloading, respectively, one can conclude that the effect of filler is stronger at loading than at retraction.

This result is confirmed by comparison of ultimate values R_∞ of parameter R_1 (which provides a measure of energy of interaction between polymer chains and inclusions under loading). A pronounced decay in R_∞ (R_∞ at $\chi = 0$ exceeds that at $\chi = 1$ wt.% by a factor of 2.7) may reflect damage of stacks of clay platelets under cyclic deformation.

The coefficients A_1 and A_2 that describe reduction in R_1 and R_2 with plastic strain adopt similar values (A_1 at $\chi = 1$ exceeds that at $\chi = 0$ wt.% by 42%, while A_2 at $\chi = 0$ is higher than A_2 at $\chi = 1$ wt.% by 32%). However, if the decrease in R_1 and R_2 is analyzed as functions of n, the situation changes dramatically: after 16 cycles of loading–retraction, R_1 at $\chi = 0$ exceeds that at $\chi = 1$ wt.% by a factor of 3.3, whereas R_2 at $\chi = 1$ exceeds that at $\chi = 0$ wt.% by a factor of 2.5.

These estimates lead to the conclusion that strong enhancement of fatigue resistance due to reinforcement may be ascribed to (i) a substantial growth of rates of plastic flow in stacks of platelets which induces (ii) noticeable reduction in the energy of interaction between polymer chains and inclusions.

6 CONCLUDING REMARKS

Observations have been reported on polypropylene/nanoclay hybrids with various concentrations of filler in tensile cyclic tests with a stress–controlled program. Reinforcement of polypropylene with nanoclay resulted in strong (by several times) reduction in ratcheting strain. Although substantial enhancement of fatigue resistance was observed at all experimental conditions, the most pronounced improvement of mechanical properties was reached when concentration of nanoclay equaled 1 wt.% at the highest value of maximum stress $\sigma^{\max} = 30$ MPa.

A constitutive model has been developed in cyclic viscoelastoplasticity of polymer nanocomposites. With reference to the homogenization concept, a nanocomposite is treated as an equivalent polymer network with two characteristic features: (i) the plastic strain tensor is split into the sum of two components that obey different flow rules, and (ii) the strain energy density equals the sum of strain energies of individual chains and the energy of interaction between chains and stacks of clay platelets.

Stress–strain relations are derived by using the Clausius–Duhem inequality. Adjustable parameters in the constitutive equations are found by fitting the experimental data (16 cycles of loading–unloading for each set of observations). The model correctly describes the stress–strain diagrams and evolution of maximum $\epsilon^{\max}$ and minimum $\epsilon^{\min}$ strains per cycle with number of cycles n.

Comparison of material constants for polymer/clay hybrids leads to a conclusion that enhancement of fatigue resistance may be attributed to acceleration of plastic flow in clusters of nanoclay which induces noticeable reduction in the energy of interaction between polymer chains and inclusions.

Acknowledgment

Financial support by the European Commission through project Nanotough–213436 is gratefully acknowledged.

REFERENCES

[1] Tjong, S.C. Structural and mechanical properties of polymer nanocomposites. *Mater. Sci. Eng. R* (2006) **53**: 73–197.

[2] Pavlidou, S. and Papaspyrides, C.D. A review on polymer–layered silicate nanocomposites. *Progr. Polym. Sci.* (2008) **33**: 1119–1198.

[3] Jancar, J., Douglas, J.F., Starr, F.W., Kumar, S.K., Cassagnau, P., Lesser, A.J., Sternstein, S.S., and Buehler, M.J. Current issues in research on structure-property relationships in polymer nanocomposites. *Polymer* (2010) **51**: 3321–3343.

[4] Yang, J.-L., Zhang, Z., Schlarb, A.K., and Friedrich, K. On the characterization of tensile creep resistance of polyamide 66 nanocomposites. Part I. Experimental results and general discussions. *Polymer* (2006) **47**: 2791–2801.

[5] Lietz, S., Yang, J.-L., Bosch, E., Sandler, J.K.W., Zhang, Z., and Altstadt, V. Improvement of the mechanical properties and creep resistance of SBS block copolymers by nanoclay filler. *Macromol. Mater. Eng.* (2007) **292**: 23–32.

[6] Drozdov, A.D., Hog Lejre, A.-L., and Christiansen, J.deC. Viscoelasticity, viscoplasticity, and creep failure of polypropylene/clay nanocomposites. *Compos. Sci. Technol.* (2009) **69**: 2596–2603.

[7] Wang, Z.D. and Zhao, X.X. Modeling and characterization of viscoelasticity of PI/SiO_2 nanocomposite films under constant and fatigue loading. *Mater. Sci. Eng. A* (2008) **486**: 517–527.

[8] Wang, Z.D. and Zhao, X.X. Creep resistance of PI/SiO_2 hybrid thin films under constant and fatigue loading. *Composites A* (2008) **39**: 439–447.

[9] Drozdov, A.D. and Christiansen, J.deC. Cyclic viscoplasticity of high-density polyethylene: Experiments and modeling. *Comput. Mater. Sci.* (2007) **39**: 465–480.

[10] Bari, S. and Hassan, T. An advancement in cyclic plasticity modeling for multiaxial ratcheting simulation. *Int. J. Plasticity* (2002) **18**: 873–894.

[11] Xia, Z., Shen, X., and Ellyin, F. An assessment of nonlinearly viscoelastic constitutive models for cyclic loading: The effect of a general loading/unloading rule. *Mech. Time-Dependent Mater.* (2005) **9**: 281–300.

[12] Tanaka, F. and Edwards, S.F. Viscoelastic properties of physically cross-linked networks. Transient network theory. *Macromolecules* (1992) **25**: 1516–1523.

[13] Derrida, B. Random-energy model: limit of a family of disordered models. *Phys. Rev. Lett.* (1980) **45**: 79–92.

[14] Drozdov, A.D. Cyclic viscoelastoplasticity and low-cycle fatigue of polymer composites. *Int. J. Solids Struct.* (2011) **48**: 2026–2040.

[15] Chaboche, J.L. A review of some plasticity and viscoplasticity constitutive theories. *Int. J. Plasticity* (2008) **24**: 1642–1693,

[16] Kang, G. Ratchetting: Recent progresses in phenomenon observation, constitutive modeling and application. *Int. J. Fatigue* (2008) **30**: 1448–1472.

[17] Sai, K. Multi-mechanism models: Present state and future trends. *Int. J. Plasticity* (2011) **27**: 250–281.